

as  $6.3 \text{ J K}^{-1} \text{ mol}^{-1}$ , and  $\Delta_f H^\circ$  may deviate by  $12.6 \text{ kJ mol}^{-1}$ .

The value of a particular standard thermodynamic property of an alkylbenzene isomer group at a specified temperature and for a specified carbon number is given by the vector product of a column in Table V and a characteristic vector in which the terms depend on temperature and carbon number. Once the 12 parameters for an isomer group and the five parameters each for graphite and molecular hydrogen have been determined, then any chemical thermodynamic property in the range 298.15–1000 K and for a desired carbon number can be computed by using a short computer program for performing the vector multiplication that

is involved. For use on a microcomputer, short programs for calculating each standard thermodynamic property in the desired language can be written so that values at the desired carbon number and temperature can be calculated by using only the data in Table V.

**Acknowledgment.** This research was supported by a grant from Basic Energy Sciences of the Department of Energy (Grant No. DE-FG02-85ER13454).

**Registry No.**  $\text{C}_6\text{H}_6$ , 71-43-2;  $\text{C}_7\text{H}_8$ , 108-88-3;  $\text{C}_9\text{H}_{10}$ , 100-41-4;  $\text{C}_9\text{H}_{12}$ , 103-65-1;  $\text{C}_{10}\text{H}_{14}$ , 104-51-8;  $\text{C}_{11}\text{H}_{16}$ , 538-68-1;  $\text{C}_{12}\text{H}_{18}$ , 1077-16-3.

## Reactions of $\text{Co}^+$ , $\text{Ni}^+$ , and $\text{Cu}^+$ with Cyclopropane and Ethylene Oxide. Metal–Methylidene Ion Bond Energies

Ellen R. Fisher and P. B. Armentrout<sup>\*,†</sup>

Department of Chemistry, University of Utah, Salt Lake City, Utah 84112 (Received: June 6, 1989)

The reactions of atomic cobalt, nickel, and copper ions with cyclopropane and ethylene oxide have been studied by using guided ion beam mass spectrometry. A predominant process in all these systems is formation of  $\text{MCH}_2^+$ . Analyses of these endothermic reactions yield the bond energies  $D^\circ(\text{Co}^+-\text{CH}_2) = 77.5 \pm 2.3 \text{ kcal/mol}$ ,  $D^\circ(\text{Ni}^+-\text{CH}_2) = 75.2 \pm 1.8 \text{ kcal/mol}$ , and  $D^\circ(\text{Cu}^+-\text{CH}_2) = 63.9 \pm 1.6 \text{ kcal/mol}$ . Differences between these values and those derived from earlier studies for  $\text{Co}^+$  and  $\text{Ni}^+$  are discussed. In addition to  $D^\circ(\text{M}^+-\text{CH}_2)$ , bond energies for  $\text{Co}^+-\text{H}$ ,  $\text{M}-\text{H}$  ( $\text{M} = \text{Co}, \text{Ni}, \text{Cu}$ ) and  $\text{M}^+-\text{O}$  and  $\text{M}-\text{O}$  ( $\text{M} = \text{Co}, \text{Ni}$ ) are evaluated and lower limits are placed on  $D^\circ(\text{M}^+-\text{C}_2\text{H}_4)$  and  $D^\circ(\text{M}^+-\text{C}_2\text{H}_2)$  ( $\text{M} = \text{Co}, \text{Ni}, \text{Cu}$ ). The reaction mechanism for these reactions is also discussed in detail.

### Introduction

Transition-metal methylidenes have long been postulated as intermediates in a variety of reactions such as metal alkyl decomposition, polymerization of olefins, olefin homologation and metathesis, and cyclopropane formation from olefins. Consequently, the bond strengths of transition-metal methylidenes are of fundamental interest in surface chemistry, organometallic chemistry, and catalysis.<sup>1</sup>

Recently we analyzed the periodic trends in the metal methylidene ion bond energies for first-row transition metals.<sup>2</sup> A reasonable correlation was discovered between these values and the promotion energy needed to put the metal ion into an appropriate electronic state for forming a double bond. However, the experimental values for  $D^\circ(\text{Co}^+-\text{CH}_2)$  and  $D^\circ(\text{Ni}^+-\text{CH}_2)$  were noticeably different than the values of  $\sim 72 \text{ kcal/mol}$  suggested by the correlation. These values,  $85 \pm 7$  and  $86 \pm 7 \text{ kcal/mol}$ , respectively, come from previous ion beam studies of the title reactions and the reaction of  $\text{M}^+$  with ethene.<sup>3,4</sup> In addition,  $D^\circ(\text{Co}^+-\text{CH}_2) = 84 \pm 5 \text{ kcal/mol}$  has been reported from photodissociation studies of  $\text{CoCH}_2^+$ .<sup>5</sup>

Because of the discrepancy with the periodic trends correlation, we undertook the present work to reinvestigate the reactions of  $\text{Co}^+$  and  $\text{Ni}^+$  with  $\text{c-C}_3\text{H}_6$  and  $\text{c-C}_2\text{H}_4\text{O}$  and to extend the measurements to  $\text{Cu}^+$ . The emphasis of the present study is to reevaluate the  $\text{MCH}_2^+$  bond energies where  $\text{M} = \text{Co}$  and  $\text{Ni}$ , and to provide the first determination for  $\text{M} = \text{Cu}$ . We also determine thresholds for other endothermic reactions, which are discussed briefly. As we shall see, the improved guided ion beam technology currently available in our laboratories allows a more definitive assessment of the thermochemistry of these reactions.

### Experimental Section

**General.** The ion beam apparatus used in these experiments has been described in detail elsewhere.<sup>6</sup> Cobalt, nickel, and copper

ions are produced as described below. The ions are extracted from the source, accelerated, and focused into a magnetic sector momentum analyzer for mass analysis. For these experiments,  $^{59}\text{Co}$  (100% natural abundance),  $^{58}\text{Ni}$  (67.77% natural abundance), and  $^{63}\text{Cu}$  (69.1% natural abundance) isotopes were used. The mass-selected ions are decelerated to a desired kinetic energy and focused into an octopole ion guide. The octopole passes through a reaction cell filled with the neutral reactant. Pressures of the gases are maintained at sufficiently low levels (0.02–0.08 mTorr) so that multiple ion–molecule reactions are improbable. The octopole ion guide ensures efficient collection of all ionic products and transmitted reactant ions. After exiting the reaction cell, the ions are extracted from the octopole, focused into a quadrupole mass filter for mass analysis, and detected by using a scintillation ion detector and standard ion counting techniques. Raw ion intensities are then converted into absolute reaction cross sections as described in detail previously.<sup>6</sup> The uncertainties in these cross sections are estimated at  $\pm 20\%$ .

Laboratory ion energies (lab) are converted to energies in the center-of-mass frame (CM) by using the conversion  $E(\text{CM}) = E(\text{lab})M/(m + M)$ , where  $m$  is the ion mass and  $M$  is the target molecule mass. The absolute energy scale and the corresponding full width at half-maximum (fwhm) of the ion kinetic energy distribution is determined by using the octopole beam guide as a retarding potential analyzer.<sup>6</sup> The uncertainty in the absolute energy scale is 0.05 eV (lab). The distribution of ion energies is Gaussian with an average fwhm of 0.7 eV (lab) for all three ions. The thermal motion of the gas in the reaction cell contributes an uncertainty of  $\sim 0.4 E_{\text{CM}}^{1/2}$  (eV) to the collision energy. Both

(1) Crabtree, R. H. *The Organometallic Chemistry of the Transition Metals*; Wiley: New York, 1988.

(2) Georgiadis, R.; Armentrout, P. B. *Polyhedron* **1988**, *7*, 1573–1581.

(3) Armentrout, P. B.; Beauchamp, J. L. *J. Chem. Phys.* **1981**, *74*, 2819–2826.

(4) Halle, L. F.; Armentrout, P. B.; Beauchamp, J. L. *Organometallics* **1983**, *2*, 1829–1833.

(5) Hettich, R. L.; Freiser, B. S. *J. Am. Chem. Soc.* **1986**, *108*, 2537–2540.

(6) Ervin, K. M.; Armentrout, P. B. *J. Chem. Phys.* **1985**, *83*, 166–189.

<sup>†</sup>NSF Presidential Young Investigator, 1984–1989. Alfred P. Sloan Fellow. Camille and Henry Dreyfus Teacher–Scholar, 1987–1992.

TABLE I: Low-Lying States of Co<sup>+</sup>, Ni<sup>+</sup>, and Cu<sup>+</sup>

ion	state	config	<i>J</i> <sup>a</sup>	<i>E</i> <sub><i>i</i></sub> <sup>b</sup> , eV	population <sup>c</sup>
Co <sup>+</sup>	a <sup>3</sup> F	3d <sup>8</sup>	4	0.000	0.520 ± 0.016
			3	0.117	0.220 ± 0.001
			2	0.198	0.104 ± 0.002
			av	0.055	0.844 ± 0.013
			5	0.415	0.076 ± 0.002
	a <sup>5</sup> F	4s3d <sup>7</sup>	4	0.499	0.040 ± 0.001
			3	0.565	0.022 ± 0.001
			2	0.613	0.013 ± 0.001
			1	0.645	0.006 ± 0.002
			av	0.483	0.157 ± 0.013
Ni <sup>+</sup>	b <sup>3</sup> F	4s3d <sup>7</sup>	av	1.298	0.002 ± 0.0001
			2.5	0.000	0.784 ± 0.020
	a <sup>2</sup> D	3d <sup>9</sup>	1.5	0.186	0.204 ± 0.010
			av	0.038	0.988 ± 0.005
Cu <sup>+</sup>	a <sup>4</sup> F	4s3d <sup>8</sup>	av	1.159	0.012 ± 0.005
	a <sup>2</sup> F	4s3d <sup>8</sup>	av	1.756	<<0.001
	a <sup>1</sup> S	3d <sup>10</sup>	0	0.000	1.000
	a <sup>3</sup> D	4s3d <sup>9</sup>	av	2.808	<<0.001
	a <sup>1</sup> D	4s3d <sup>9</sup>	2	3.257	

<sup>a</sup> Statistical average over all *J* levels except where noted. <sup>b</sup> Energies are taken from: Sugar, J.; Corliss, C. *J. Phys. Chem. Ref. Data* **1985**, *14*, Suppl. 2. <sup>c</sup> Maxwell-Boltzmann distribution at 2250 ± 100 K.

effects are taken into account when analyzing the experimental results.<sup>6</sup> At very low ion energies, the slower ions in the ion beam energy distribution are not transmitted through the octopole, which results in a narrowing of the ion energy distribution. The CM frame energies in the data plots are mean ion energies taking into account the truncation of the Gaussian ion beam distribution. Because of this effect, we are able to measure cross sections at energies below one fwhm of the beam energy spread. Details of this data analysis have been discussed previously.<sup>6,7</sup>

**Ion Source.** The metal ions are produced by surface ionization (SI). In the SI source, CoCl<sub>2</sub>·6H<sub>2</sub>O, NiCl<sub>2</sub>·6H<sub>2</sub>O, or CuBr<sub>2</sub> is dehydrated and sublimed in a resistively heated oven. The vapor is directed at a rhenium filament which is resistively heated to 2250 ± 100 K as measured by optical pyrometry. The metal complex decomposes on the filament and metal ions are produced by surface ionization of the resulting metal atoms. If we presume that the metal atom reaches equilibrium at the filament temperature before desorption, the electronic state distribution of the beam produced by SI should have a Maxwell-Boltzmann distribution (Table I). Previous studies<sup>8</sup> in our lab on other systems indicate that this is a reasonable assumption.

CoCl<sub>2</sub>·6H<sub>2</sub>O, NiCl<sub>2</sub>·6H<sub>2</sub>O, and CuBr<sub>2</sub> are obtained from Mallinckrodt. Cyclopropane and ethylene oxide are obtained from Matheson (99.99% purity) and are used without further purification except for multiple freeze-pump-thaw cycles.

**Thermochemical Analysis.** Cross sections for endothermic reactions of species having a distribution of electronic states, denoted by *i*, can be analyzed by using eq 1, which involves an

$$\sigma(E) = \sum_i g_i \sigma_{i0} (E - E_0 + E_i)^n / E^m \quad (1)$$

explicit sum of the contributions of individual states weighted by their populations, *g<sub>i</sub>*. Here, *E*<sub>0</sub> is the threshold for reaction of the lowest electronic level of the ion, *E<sub>i</sub>* is the electronic excitation of each particular *J* level, *σ*<sub>*i0*</sub> is an energy-independent scaling factor, and *n* and *m* are parameters which depend on the theoretical model being used.

In the Co<sup>+</sup> systems, the <sup>3</sup>F ground state and the <sup>5</sup>F first excited state (Table I) were included in the analysis with the *J* levels resolved. For the Ni<sup>+</sup> systems, the individual *J* levels of the <sup>2</sup>D ground state and an average for the <sup>4</sup>F excited state were included in the analysis (Table I). The surface ionization source produces essentially pure ground state Cu<sup>+</sup>(<sup>1</sup>S) (>99.9%); therefore, eq 1 has only a single term for Cu<sup>+</sup>. In the absence of information

TABLE II: Literature Thermochemistry<sup>a</sup> (298 K) (in kcal/mol)

species	$\Delta_f H$	species	$\Delta_f H$
H	52.1	CH <sub>2</sub> =CHCH <sub>2</sub>	39 <sup>b</sup>
CH <sub>2</sub>	92.35 ± 1.0	CH <sub>2</sub> =CHCH <sub>2</sub> <sup>+</sup>	226.0 <sup>d</sup>
CH <sub>4</sub>	-17.9 ± 0.1	c-C <sub>3</sub> H <sub>6</sub>	12.74 ± 0.14 <sup>c</sup>
C <sub>2</sub> H <sub>2</sub>	54.2 ± 0.2	O	59.55 ± 0.02
C <sub>2</sub> H <sub>4</sub>	12.5 ± 0.1	H <sub>2</sub> O	-57.80 ± 0.01
C <sub>2</sub> H <sub>4</sub> <sup>+</sup>	254.8 ± 0.2 <sup>d</sup>	CO	-26.42 ± 0.04
c-C <sub>3</sub> H <sub>3</sub>	105 ± 4 <sup>b</sup>	H <sub>2</sub> CO	-25.96 ± 0.12 <sup>c</sup>
c-C <sub>3</sub> H <sub>3</sub> <sup>+</sup>	257 <sup>d</sup>	CH <sub>3</sub> CO <sup>+</sup>	156 <sup>d</sup>
c-C <sub>3</sub> H <sub>5</sub>	66.9 <sup>b</sup>	c-C <sub>2</sub> H <sub>3</sub> O <sup>+</sup>	201 <sup>d</sup>
c-C <sub>3</sub> H <sub>5</sub> <sup>+</sup>	255 <sup>d</sup>	c-C <sub>2</sub> H <sub>4</sub> O	-12.57 ± 0.14 <sup>c</sup>
Co	102 <sup>d</sup>	Co <sup>+</sup>	283 <sup>d</sup>
Ni	102.8 <sup>d</sup>	Ni <sup>+</sup>	278.9 <sup>d</sup>
Cu	80.9 <sup>d</sup>	Cu <sup>+</sup>	259.0 <sup>d</sup>

<sup>a</sup> All values except where noted are from Chase, M. W., et al. *J. Chem. Phys. Ref. Data* **1985**, *14*, Suppl. No. 1 (JANAF Tables). <sup>b</sup> McMillen, D. F.; Golden, D. M. *Annu. Rev. Phys. Chem.* **1982**, *33*, 493-532. <sup>c</sup> Pedley, J. M.; Naylor, R. D.; Kirby, S. P. *Thermochemical Data of Organic Compounds*; Chapman and Hall: London, 1986. <sup>d</sup> Reference 38.

to the contrary, we assume that *n*, *m*, and *σ*<sub>*i0*</sub> in eq 1 are the same for all states. Errors in threshold values are determined by the variation in *E*<sub>0</sub> for the various models applied to several data sets, and the absolute uncertainty in the energy scale, ~0.02 eV.

In this study, eq 1 is evaluated for the cases where *m* = 1 for each endothermic reaction channel. The parameters *n*, *σ*<sub>*i0*</sub>, and *E*<sub>0</sub> are allowed to vary freely to best fit the data as determined by nonlinear least-squares analysis. This general form and its ability to reproduce the data has been discussed previously.<sup>9</sup> A value of *m* = 1 is chosen because this form has been derived as a model for translationally driven reactions<sup>10</sup> and has been found to be quite useful in describing the shapes of endothermic reaction cross sections and in deriving accurate thermochemistry for a wide range of systems.<sup>9,11,12</sup>

The reaction cross section for an endothermic process may decline at higher energies due to dissociation of the product ion. For such systems, cross sections are analyzed by using a model previously outlined which makes a simple statistical assumption within the constraints of angular momentum conservation.<sup>13</sup> For this model, there are two parameters which are allowed to optimize: *E<sub>D</sub>*, which is the energy at which dissociation begins, and *p*, which is related to the number of degrees of freedom in the transition state.

Heats of formation used in deriving thermochemical results are given in Table II. We assume that the neutral reactants and the products formed at the threshold of an endothermic reaction are characterized by a temperature of 298 K in all degrees of freedom. Thus, we make no correction for the energy available in internal modes of the neutral reactant. Furthermore, eq 1 implicitly assumes that there are no activation barriers in excess of the endothermicity. This assumption is generally true for ion-molecule reactions and has been explicitly tested a number of times.<sup>11-14</sup> We have previously discussed the limitations on converting threshold energies, *E*<sub>0</sub>, to metal ion-ligand bond energies.<sup>9</sup> In this study, the bond energies are measured in both systems to avoid systematic errors and the effects of activation barriers and kinetic shifts.

(9) (a) Aristov, N.; Armentrout, P. B. *J. Am. Chem. Soc.* **1986**, *108*, 1806-1819. (b) Sunderlin, L. S.; Aristov, N.; Armentrout, P. B. *J. Am. Chem. Soc.* **1987**, *109*, 78-89.

(10) Chesnavich, W. J.; Bowers, M. T. *J. Phys. Chem.* **1979**, *83*, 900-905.

(11) Boo, B. H.; Armentrout, P. B. *J. Am. Chem. Soc.* **1987**, *109*, 3549-3559.

(12) Weber, M. E.; Armentrout, P. B. *J. Chem. Phys.* **1988**, *88*, 6898-6910.

(13) Weber, M. E.; Elkind, J. L.; Armentrout, P. B. *J. Chem. Phys.* **1986**, *84*, 1521-1529.

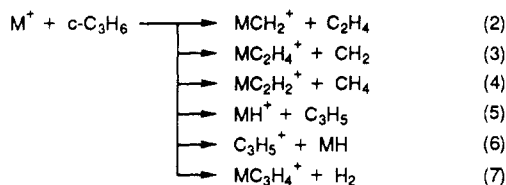
(14) (a) Ervin, K. M.; Armentrout, P. B. *J. Chem. Phys.* **1986**, *84*, 6738-6749. (b) Boo, B. H.; Armentrout, P. B. *J. Am. Chem. Soc.* **1987**, *109*, 3549-3559. (c) Ervin, K. M.; Armentrout, P. B. *J. Chem. Phys.* **1987**, *86*, 2659-2673. (d) Elkind, J. L.; Armentrout, P. B. *J. Phys. Chem.* **1984**, *88*, 5454-5456.

(7) Ervin, K. M.; Armentrout, P. B.; *J. Chem. Phys.* **1987**, *86*, 2659-2673.

(8) Sunderlin, L. S.; Armentrout, P. B. *J. Phys. Chem.* **1988**, *92*, 1209-1219.

## Results

**Cyclopropane.**  $\text{Co}^+$ ,  $\text{Ni}^+$ , and  $\text{Cu}^+$  react with cyclopropane to form a variety of products. The major products, formed in reactions 2–7, are similar for all three ions, although there are some notable differences.



$\text{Co}^+ + \text{c-C}_3\text{H}_6$ . The cross sections for all major products in the reaction of  $\text{Co}^+$  with cyclopropane are shown in Figure 1a. The principle reaction observed is formation of the cobalt methylidene ion, reaction 2. The cross section for  $\text{CoCH}_2^+$  rises quickly and levels out at about  $4 \text{ \AA}^2$  at low energy. It then begins to decrease at about  $D^\circ(\text{C}_2\text{H}_4\text{-CH}_2) = 3.99 \text{ eV}$ . Our results for reaction 2 are in rough agreement with those of Armentrout and Beauchamp (AB).<sup>3</sup> Their cross-section magnitude rises sharply from a nonzero value at their lowest kinetic energies to a sharp peak of  $\sim 7 \text{ \AA}^2$  at  $\sim 1.5 \text{ eV}$ , before decreasing rapidly to a magnitude below our results at higher energies.<sup>15</sup> The magnitude and shape of the data shown here have been reproduced on several occasions over the course of a year and should be accurate within our experimental error limits of  $\pm 20\%$ .

The cross sections for the products of reactions 3–7 are significantly smaller than that for reaction 2. AB commented on the presence of these products (except for  $\text{CoH}^+$ ) but could not obtain reasonable data for them due to their small magnitudes. The cross section for reaction 3 peaks at about the same energy as reaction 2,  $\approx 4 \text{ eV}$ , consistent with the neutral bond energy as well as competition between these two channels. Identification of the neutral products in reaction 4 is somewhat uncertain ( $\text{CH}_2 + \text{H}_2$  is a possibility), but thermochemical arguments (detailed below) establish that  $\text{CH}_4$  is produced at threshold.

Formation of both  $\text{CoH}^+$  and  $\text{C}_3\text{H}_5^+$  are seen at higher energies. These two products have similar shapes and similar apparent thresholds of  $\sim 3 \text{ eV}$ , although more  $\text{CoH}^+$  than  $\text{C}_3\text{H}_5^+$  is formed at all energies examined. Formation of  $\text{C}_3\text{H}_3^+$  is also observed and is presumed to be due to decomposition of the primary alkyl ion product,  $\text{C}_3\text{H}_5^+$ . The dehydrogenation product,  $\text{CoC}_3\text{H}_4^+$ , formed in reaction 7, is not shown in Figure 1a. The cross-section magnitude below  $3 \text{ eV}$  for this product does not exceed  $0.10 \text{ \AA}^2$ , and the magnitude above  $3 \text{ eV}$  is close to the detection limit in this study,  $0.01 \text{ \AA}^2$ . The only other product that we observe (not shown in Figure 1a) is the adduct,  $\text{CoC}_3\text{H}_6^+$ , which is a collisionally stabilized complex as established by the pressure dependence of its cross section (over a pressure range of  $0.02\text{--}0.20 \text{ mTorr}$ ).

$\text{Ni}^+ + \text{c-C}_3\text{H}_6$ . The reactions of  $\text{Ni}^+$  with  $\text{c-C}_3\text{H}_6$ , Figure 1b, are much like those of  $\text{Co}^+$ . The major difference is that reactions 5 and 7 are not seen. Formation of  $\text{NiCH}_2^+$ , process 2, is again the dominant reaction. The cross section for this process is similar to both size and shape to that from the  $\text{Co}^+$  reaction, although the threshold for reaction occurs at a higher energy. The results presented here for reaction 2 with  $\text{M} = \text{Ni}$  are in good qualitative agreement with those of Halle, Armentrout, and Beauchamp<sup>4</sup> (HAB) for the same reaction. (These authors do not report any other processes in this system.) The cross section for reaction 3 peaks at about the same energy as reaction 2,  $\sim 4 \text{ eV}$ , consistent with the neutral bond energy as well as competition between these two channels.

Reaction 4, formation of  $\text{NiC}_2\text{H}_2^+$ , must again be accompanied by  $\text{CH}_4$  neutral as established by thermochemical arguments below.  $\text{C}_3\text{H}_5^+$  and  $\text{C}_3\text{H}_3^+$  cross sections are comparable in size and shape to those seen in the  $\text{Co}^+$  system but are observed to

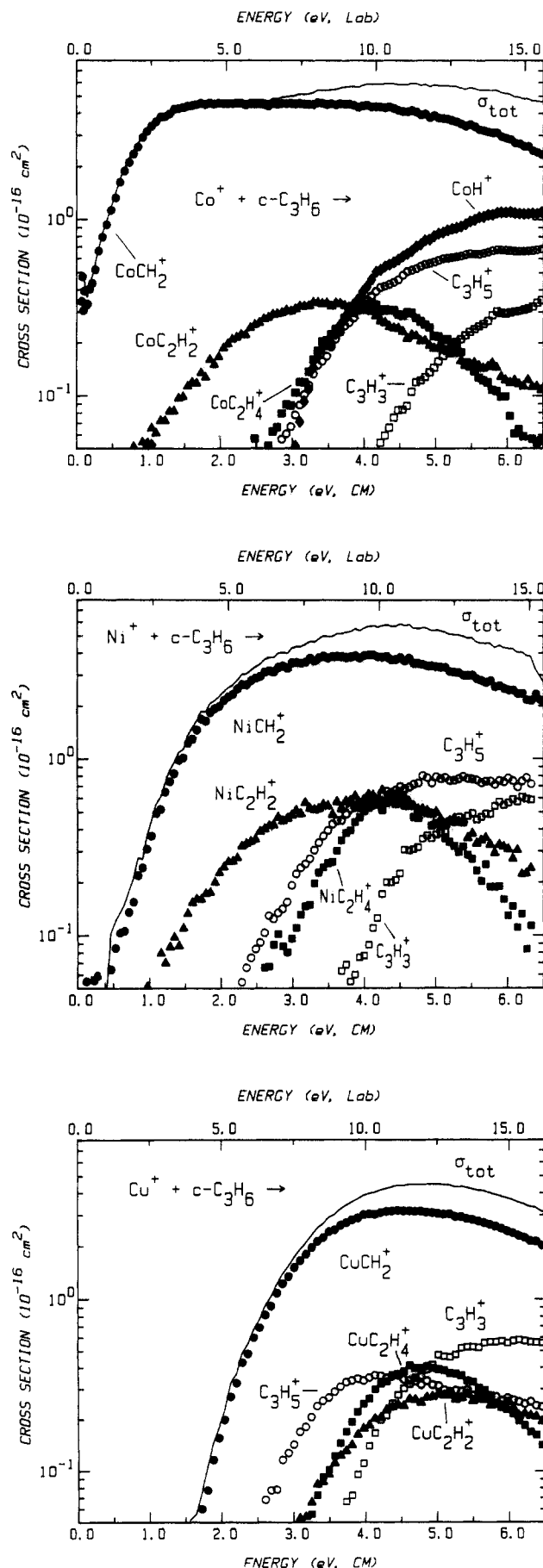


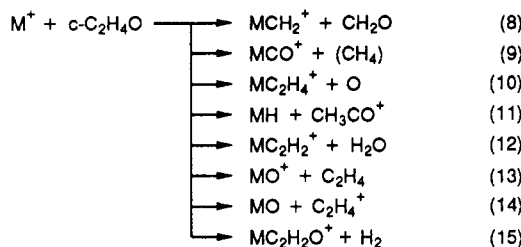
**Figure 1.** Variation of product cross sections with translational energy in the center-of-mass frame of reference (lower scale) and the laboratory frame (upper scale) for reaction of cyclopropane with  $\text{Co}^+$  (part a, top),  $\text{Ni}^+$  (part b, middle), and  $\text{Cu}^+$  (part c, bottom).

(15) The differences in shape and magnitude could be a result of attenuation of the ion beam in AB's experiments since the cross section is directly related to the ratio of the product ion intensity to the reactant ion intensity.<sup>6</sup> The octopole ion guide helps prevent such distortions.

have lower thresholds by  $\sim 0.5$  eV compared to the cobalt system. The only other product that we observe in this system (not shown in Figure 1b) is the adduct,  $\text{NiC}_3\text{H}_6^+$ , which is again a collisionally stabilized complex as established by the pressure dependence of its cross section (over a pressure range of 0.02–0.15 mTorr).

$\text{Cu}^+ + c\text{-C}_3\text{H}_6$ . The reactions of  $\text{Cu}^+$  with  $c\text{-C}_3\text{H}_6$  are much like those of  $\text{Ni}^+$  (Figure 1c). Again, process 2 is the dominant reaction, and reactions 5 and 7 are not seen. In addition, formation of the adduct ion is not seen. The threshold for reaction 2 is much higher in energy than with either  $\text{Co}^+$  or  $\text{Ni}^+$ . The cross section for formation of  $\text{CuCH}_2^+$  rises slowly from threshold, and peaks slightly higher than the neutral bond energy, but is similar in shape to that from reaction 2 with  $M = \text{Ni}$ . While not obvious in Figure 1c, the apparent threshold for reaction 4 is well below that for reaction 3, which again means that  $\text{CH}_4$  is the neutral product in the former reaction. The alkyl ions have thresholds only slightly lower than those observed in the Ni system.

**Ethylene Oxide.** The metal ions studied here react with ethylene oxide to form a variety of products. The major products, formed in reactions 8–15, are somewhat similar to  $M = \text{Co}$  and



Ni, but there are some notable differences with  $M = \text{Cu}$ . Most of these reactions find analogy with the products observed in the cyclopropane system.

$\text{Co}^+ + c\text{-C}_2\text{H}_4\text{O}$ .  $\text{Co}^+$  reacts with ethylene oxide to form all products of reactions 8–15. The major products are shown in Figure 2a. Other minor products not shown in Figure 2a include  $\text{CoHCO}^+$  and  $\text{CoOH}^+$ . Both of these products have maximum cross sections of  $<0.5 \text{ \AA}^2$  which decrease with increasing energies, indicating exothermic reactions. In addition to reactions 8–15,  $\text{Co}^+$  also reacts efficiently to form the adduct  $\text{CoC}_2\text{H}_4\text{O}^+$ . It was verified that adduct formation is *not* the result of collisional stabilization by determining that the cross section shown in Figure 2a is independent of the reactant neutral pressure (over a pressure range of 0.01–0.14 mTorr).

Again, it is formation of  $\text{CoCH}_2^+$ , reaction 8, which dominates although formation of  $\text{CoCO}^+$  is nearly as probable. These cross sections are seen to decrease monotonically with increasing energy and are considerably larger than the cross section measured in the cyclopropane system. This clearly suggests that reactions 8 and 9 are exothermic. The ionic products of reactions 9 and 10 have the same mass. We identify this exothermic cross section as reaction 9, however, where the neutral product is  $\text{CH}_4$ . This is consistent with results from an analogous study<sup>16</sup> with  $\text{Cr}^+$  and with thermodynamic considerations discussed below. Reaction 11 was not observed in the  $\text{Cr}^+$  study or with  $\text{Mn}^+$ ,<sup>17</sup> but is a major product seen with  $\text{Co}^+$ .

Formation of  $\text{CoO}^+$ , reaction 13, is slightly endothermic. The cross section for this process, however, is nonzero at our lowest kinetic energy, which is most likely due to the contribution of excited electronic states of  $\text{Co}^+$  reacting exothermically to form  $\text{CoO}^+$ . This is verified by the thermochemical analysis performed below. In competition with this reaction at higher kinetic energies is reaction 14, formation of  $\text{C}_2\text{H}_4^+$  and the *neutral* metal oxide. Dehydration and dehydrogenation, reactions 12 and 15, are minor exothermic processes.

AB also studied the reactions of  $\text{Co}^+$  with ethylene oxide.<sup>3</sup> In contrast to the data in the cyclopropane system, the data presented

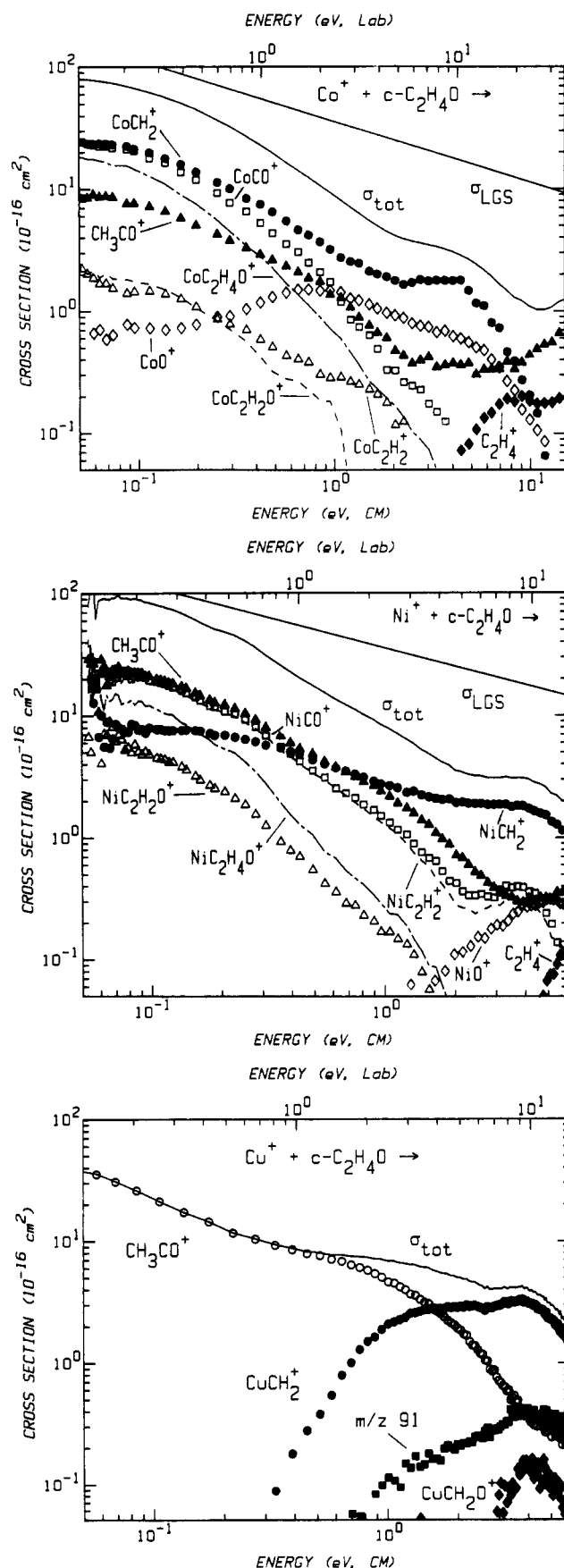


**Figure 2.** Variation of product cross sections with translational energy in the center-of-mass frame of reference (lower scale) and the laboratory frame (upper scale) for reaction of ethylene oxide with  $\text{Co}^+$  (part a, top),  $\text{Ni}^+$  (part b, middle); and  $\text{Cu}^+$  (part c, bottom). Note that the energy axis of part a differs from those in parts b and c. Closed triangles and open squares represent the  $\text{CH}_3\text{CO}^+$  and the  $\text{MCO}^+$  cross section, respectively (parts a and b).

(16) Georgiadis, R.; Armentrout, P. B. *Int. J. Mass Spectrom. Ion Processes* **1989**, *89*, 227–247.

(17) Sunderlin, L. S.; Armentrout, P. B., *J. Phys. Chem.*, submitted for publication.

by AB for the reactions with ethylene oxide compare much more favorably with the data presented here. Both the sizes and shapes of the major reaction cross sections reported by AB are within experimental error of those reported here. Those of the minor products, however, are not in as good agreement. Specifically, the magnitude of the  $\text{CoC}_2\text{H}_2^+$  and  $\text{CH}_3\text{CO}^+$  cross sections are significantly smaller than ours. In addition, the energy range included in AB's results is much narrower than ours, 0.2–4 eV, which prevented AB from observing the  $\text{C}_2\text{H}_4^+$  ion at high energies. The only other significant product not reported by AB is the adduct ion,  $\text{CoC}_2\text{H}_4\text{O}^+$ .

$\text{Ni}^+ + c\text{-C}_2\text{H}_4\text{O}$ . In the reaction of  $\text{Ni}^+$  with ethylene oxide, processes 8–15 and formation of the adduct are observed (Figure 2b). Pressure dependence studies establish that the adduct is again formed in a single bimolecular encounter (over a pressure range of 0.02–0.09 mTorr). Although the cross section resulting from reaction 8 is again quite large, it does not dominate this reaction as it did with  $\text{Co}^+$ . Instead, the largest cross sections result from reactions 9, 11, and 12, all exothermic processes. Although the  $\text{NiCH}_2^+$  cross section is nonzero at our lowest energies, its behavior is distinct from that of these exothermic ion–molecule reactions. The contrast in behavior will be shown to indicate that process 8 has a barrier, although a small one. The finite cross section at zero kinetic energy is a result of the spread in ion energies and the thermal motion of the ethylene oxide, as well as the exothermic reaction of electronically excited states of  $\text{Ni}^+$ . Similar behavior has been observed elsewhere.<sup>14c,18</sup>

Again, since the products of reactions 9 and 10 have the same mass, we identify the exothermic cross section as reaction 9, with the neutral product being  $\text{CH}_4$ . The second feature seen in this cross section (which starts about 2 eV) is likely to be  $\text{NiC}_2\text{H}_4^+$  (reaction 10).

HAB also studied the reactions of  $\text{Ni}^+$  with ethylene oxide,<sup>4</sup> but only observed reactions 8, 9, 11, 15, and formation of the adduct ion,  $\text{NiC}_2\text{H}_4\text{O}^+$ . This is in part because data was collected from only 0.5 to 2.0 eV. The magnitudes and sizes of the major products reported by HAB again compare favorably with those reported here, within experimental error, although the limited energy range prevented them from observing the distinctive behavior of the  $\text{NiCH}_2^+$  cross section.

$\text{Cu}^+ + c\text{-C}_2\text{H}_4\text{O}$ . Results for the reactions of  $\text{Cu}^+$  with ethylene oxide are very different from those of  $\text{Co}^+$  and  $\text{Ni}^+$  (Figure 2c). Clearly,  $\text{Cu}^+$  does not form nearly as many products with ethylene oxide as  $\text{Co}^+$  and  $\text{Ni}^+$  do, although the total cross section at low energies is still about 1/2 that of these other ions, and at high energies, it is somewhat larger. The dominant process seen at low kinetic energies is the exothermic formation of the acetyl ion  $\text{CH}_3\text{CO}^+$ , reaction 11. At higher kinetic energies (above  $\sim 1.5$  eV), formation of the metal methylidene ion, reaction 8, dominates. In addition, the only other processes observed are formation of the  $m/z$  91 ion and formation of  $\text{CuCH}_2\text{O}^+$ , reaction 16. Unlike



with  $\text{Co}^+$  and  $\text{Ni}^+$ , formation of the  $m/z$  91 ion is endothermic and therefore is not easily assigned to reaction 9 or 10.

### Thermochemistry

Cross sections for the endothermic reactions are subjected to detailed threshold analysis as described in the Experimental Section. Results for the reactions of the three ions,  $\text{Co}^+$ ,  $\text{Ni}^+$ , and  $\text{Cu}^+$ , are summarized in Tables III–V and discussed below. Table VI summarizes the thermochemical results for this work and related results from previous experimental and theoretical studies.

**Cobalt Methylidene Ion.**  $\text{CoCH}_2^+$  is the predominant product observed in the reactions of  $\text{Co}^+$  with both of the neutral molecules studied here. A representative fit to the experimental data for formation of  $\text{CoCH}_2^+$  from cyclopropane, reaction 2, is shown in Figure 3. Note that the reproduction of  $\sigma(\text{CoCH}_2^+)$  is excellent

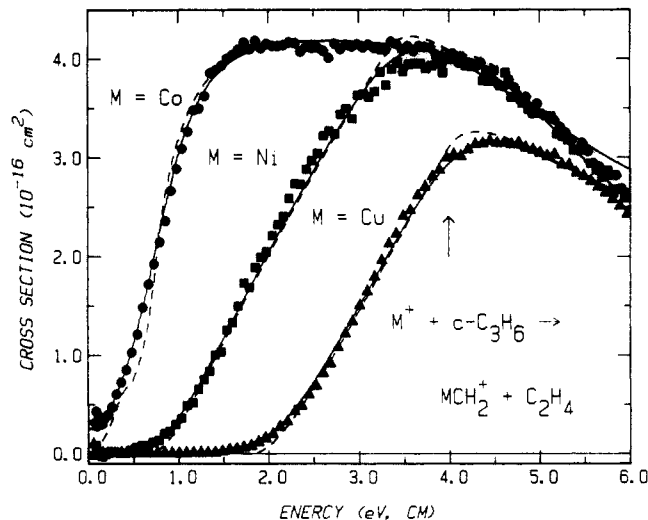


**Figure 3.** Cross sections for formation of  $\text{MCH}_2^+$  from the reaction of  $\text{M}^+$  with cyclopropane, where  $\text{M} = \text{Co}, \text{Ni},$  and  $\text{Cu}$  (same data as Figure 1). The lines are the best fits to the data using the parameters given in Tables III–V and including the high-energy model. The arrow indicates the  $\text{CH}_2\text{-C}_2\text{H}_4$  bond dissociation energy at 4.0 eV.

**TABLE III: Parameters Used in Eq 1 for Fitting  $\text{Co}^+$  Reaction Cross Sections**

ionic product	$n$	$E_0, \text{eV}$	$\sigma_0$	$p$	$E_D$
Cyclopropane					
$\text{CoCH}_2^+$	$0.7 \pm 0.1$	$0.68 \pm 0.07$	$6.10 \pm 0.09$	1	4.5
$\text{CoC}_2\text{H}_2^+$	$2.2 \pm 0.2$	$0.66 \pm 0.15$	$0.11 \pm 0.05$	3	3.0
$\text{CoC}_2\text{H}_4^+$	$2.0 \pm 0.8$	$2.27 \pm 0.19$	$0.43 \pm 0.10$	2	4.1
$\text{CoH}^+$	$1.6 \pm 0.3$	$2.60 \pm 0.15$	$1.05 \pm 0.14$	0	4.6
$\text{C}_3\text{H}_5^+$	$1.4 \pm 0.1$	$2.91 \pm 0.10$	$0.88 \pm 0.17$	1	4.2
$\text{C}_3\text{H}_3^+$	$1.5 \pm 0.1$	$3.83 \pm 0.09$	$0.46 \pm 0.06$	1	5.4
Ethylene Oxide					
$\text{CoCH}_2^+$	0.5	$0.01 \pm 0.05$	$6.5 \pm 1.0$	0	0.35
$\text{CoO}^+$	$0.6 \pm 0.2$	$0.37 \pm 0.04$	$2.22 \pm 0.36$		
$\text{C}_2\text{H}_4^+$	$0.8 \pm 0.1$	$3.78 \pm 0.08$	$0.49 \pm 0.04$		

over the entire energy range. This model includes a small contribution for the exothermic reaction of  $\text{Co}^+(\text{b}^3\text{F})$ , 1.3 eV higher in energy than the ground state (Table I).<sup>19</sup> This interpretation of reaction 2, Table III, leads to a bond energy for  $\text{CoCH}_2^+$  of  $3.31 \pm 0.08$  eV.

In the ethylene oxide system, formation of  $\text{CoCH}_2^+$  is apparently exothermic; however, the  $\text{CoCH}_2^+$  bond energy determined above suggests that reaction 8 is endothermic by  $0.11 \pm 0.08$  eV. To examine this possibility more carefully, we compare the shape of  $\sigma(\text{CoCH}_2^+)$  to that for a product formed in a reaction that is certainly exothermic. A good candidate is  $\sigma(\text{CoCO}^+)$ , since the decarbonylation reaction is exothermic by  $2.85 \pm 0.13$  eV.<sup>20,21</sup> We find that the ratio of  $\sigma(\text{CoCH}_2^+)$  to  $\sigma(\text{CoCO}^+)$  increases with increasing energy, consistent with reaction 8 being endothermic. This can be further tested by modeling these cross sections with eq 1. We find that  $\sigma(\text{CoCO}^+)$  is accurately reproduced when  $E_0 = 0$  eV,  $n = 0.5$ , and  $m = 1.0$ , a form equivalent to the Langevin–Gioumousis–Stevenson model for exothermic ion–molecule reactions.<sup>22</sup> Likewise,  $\sigma(\text{CoCH}_2^+)$  and the ratio of the two cross sections are best modeled by the same equation with  $E_0 = 0.01$  eV (Table III). If  $E_0$  is lowered to 0 eV or raised above 0.02 eV, the data are no longer reproduced. This endothermicity means that only the lowest  $J$  level of the  $^3\text{F}$  ground state is endothermic

(19) This contribution is just the LGS model scaled by the population of the  $\text{b}^3\text{F}$  state given in Table I, and an arbitrary reactivity of 1/3 to best reproduce the data.

(20) This uses the value  $D^\circ(\text{Co}^+\text{-CO}) = 1.47 \pm 0.13$  eV from ref 21.

(21) Hanratty, M. A.; Beauchamp, J. L.; Illies, A. J.; van Koppen, P.; Bowers, M. T. *J. Am. Chem. Soc.* **1988**, *110*, 1–14.

(22) Gioumousis, G.; Stevenson, D. P. *J. Chem. Phys.* **1958**, *29*, 292–299.

(18) Loh, S. K.; Fisher, E. R.; Lian, L.; Schultz, R. H.; Armentrout, P. B. *J. Phys. Chem.* **1989**, *93*, 3159–3167.

TABLE IV: Parameters Used in Eq 1 for Fitting Ni<sup>+</sup> Reaction Cross Sections

ionic product	<i>n</i>	<i>E</i> <sub>0</sub> , eV	<i>σ</i> <sub>0</sub>	<i>p</i>	<i>E</i> <sub>D</sub>
Cyclopropane					
NiCH <sub>2</sub> <sup>+</sup>	1.7 ± 0.2	0.78 ± 0.07	3.32 ± 0.41	1	3.4
NiC <sub>2</sub> H <sub>2</sub> <sup>+</sup>	1.8 ± 0.3	0.83 ± 0.19	0.38 ± 0.13	1	3.4
NiC <sub>2</sub> H <sub>4</sub> <sup>+</sup>	2.2 ± 0.3	2.49 ± 0.20	0.70 ± 0.26	3	4.2
C <sub>3</sub> H <sub>5</sub> <sup>+</sup>	1.4 ± 0.2	2.42 ± 0.18	1.11 ± 0.26		
C <sub>3</sub> H <sub>3</sub> <sup>+</sup>	1.4 ± 0.1	3.69 ± 0.13	1.28 ± 0.26		
Ethylene Oxide					
NiCH <sub>2</sub> <sup>+</sup>	0.3 ± 0.1	0.11 <sub>5</sub> ± 0.03	3.34 ± 0.57		
NiO <sup>+</sup>	1.7 ± 0.1	0.81 ± 0.08	0.14 ± 0.02	2	4.6
C <sub>2</sub> H <sub>4</sub> <sup>+</sup>	1.0 ± 0.1	3.95 ± 0.20	0.32 ± 0.07		

and that reaction of the remaining 48% of the Co<sup>+</sup> ions is exothermic. After including the uncertainty in the energy scale and variations for different data sets, the derived threshold is 0.01 ± 0.05 eV<sup>23</sup> which results in *D*<sup>0</sup>(Co<sup>+</sup>-CH<sub>2</sub>) = 3.41 ± 0.06 eV, in good agreement with the result from the cyclopropane system. This presumes that the threshold corresponds to formation of H<sub>2</sub>CO. This process is the lowest energy reaction and mechanistically is directly analogous to reaction 2. It is also possible that the neutral products in reaction 8 are H<sub>2</sub> + CO. The heats of formation of these products, however, are nearly thermoneutral with that of H<sub>2</sub>CO (0.02 eV higher) and would be formed via a distinct mechanism from reaction 2. In any case, the error limits adequately include this possibility.

Our final value for *D*<sup>0</sup>(CoCH<sub>2</sub><sup>+</sup>) is simply the average result from the two systems, 3.36 ± 0.07 eV (77.5 ± 1.6 kcal/mol). This value is closer to the predicted value of ~72 kcal/mol<sup>2</sup> and still within experimental error of the generally accepted value determined by AB in previous ion beam experiments, 3.7 ± 0.3 eV.<sup>3</sup> We note, however, these authors determined a threshold for reaction 2 of 0.5 ± 0.3 eV, but this has not been corrected for the electronic energy of the Co<sup>+</sup> beam. We note that, when AB's threshold is corrected by the average electronic energy of their beam,  $\bar{E}_i = 0.12$  eV,<sup>24</sup> their value for *E*<sub>0</sub> (=0.62 ± 0.3 eV is in good agreement with the 0.68 ± 0.07 eV threshold determined here. Also, in contrast to the present conclusion, AB reasonably decided that reaction 8 was exothermic, thus giving a lower limit of 3.42 eV for the Co<sup>+</sup>-CH<sub>2</sub> bond energy. The final value reported by AB actually comes from results for the reaction of cobalt ions with ethene. If we again correct for the electronic energy of the Co<sup>+</sup>, AB's result for this reaction yields *D*<sup>0</sup>(Co<sup>+</sup>-CH<sub>2</sub>) = 3.55 ± 0.3 eV, in agreement with the present value.

Other determinations of the Co<sup>+</sup>-CH<sub>2</sub> bond energy have been reported by Freiser and co-workers. Hettich and Freiser<sup>5</sup> report *D*<sup>0</sup>(Co<sup>+</sup>-CH<sub>2</sub>) = 3.65 ± 0.2 eV (84 ± 5 kcal/mol) based on photodissociation studies of CoCH<sub>2</sub><sup>+</sup>. We note that these authors had difficulty in assigning a definitive photodissociation threshold due to internally excited ions. It is clear from their results, however, that the CoCH<sub>2</sub><sup>+</sup> bond energy must lie between 3.18 and 3.65 eV (corresponding to thresholds of 390 and 340 nm, respectively). Forbes, Lech, and Freiser<sup>25</sup> studied reaction 2 using FTMS and found a threshold of 0.38 eV which they approximately corrected to 0.53 ± 0.3 eV, although no correction for electronic excitation was made. Their resulting CoCH<sub>2</sub><sup>+</sup> bond energy of 3.5 ± 0.3 eV is within experimental error of our value. These authors also obtain a bond energy of 3.2 ± 0.8 eV from a similar analysis of the reaction of Co<sup>+</sup> + ethene.

**Nickel Methylidene Ion.** For Ni<sup>+</sup> + cyclopropane, the cross section for reaction 2 is similar to that for the Co<sup>+</sup> system (Figure

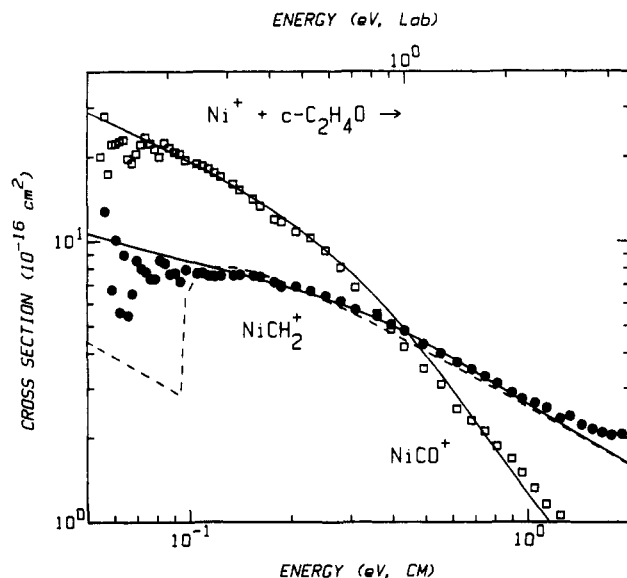


Figure 4. Cross sections for reaction 8 (closed circles) and reaction 9 (open squares) with M = Ni (same data as Figure 2b). Solid lines are the fits to these data channels described in the text after convoluting over the experimental energy distributions. The dashed line is the unconvoluted fit to the NiCH<sub>2</sub><sup>+</sup> data.

3). Thus, the analysis of this data was directly analogous in both systems. The best fit to both the threshold region and the high-energy behavior is shown in Figure 3, with the parameters given in Table IV. This analysis results in a threshold that is 0.1 eV higher than that for Co<sup>+</sup> and thus *D*<sup>0</sup>(Ni<sup>+</sup>-CH<sub>2</sub>) = 3.21 ± 0.08 eV.

In the ethylene oxide system, reaction 8 with Ni<sup>+</sup> is endothermic. This immediately places an upper limit on the Ni<sup>+</sup>-CH<sub>2</sub> bond energy, *D*<sup>0</sup>(Ni<sup>+</sup>-CH<sub>2</sub>) ≤ 3.42 eV = *D*<sup>0</sup>(CH<sub>2</sub>-CH<sub>2</sub>O). More specific information can be obtained by analyzing this cross section as described above. It is found that eq 1 reproduces the data with the parameters given in Table IV. This fit is shown in Figure 4. The derived threshold of 0.11 ± 0.03 eV implies that only the reaction of Ni<sup>+</sup>(<sup>2</sup>D<sub>5/2</sub>), the lowest *J* level, is actually endothermic while Ni<sup>+</sup>(<sup>2</sup>D<sub>3/2</sub>) reacts exothermically. The unconvoluted fit to the data shown in Figure 4 explicitly depicts the difference in reactivity of these two states. To verify that this cross section behavior differs from that for an exothermic reaction, we also analyzed the data for reaction 9, a process which is certainly exothermic for both *J* states. As shown in Figure 4, the data for this reaction is accurately reproduced by using eq 1 with a form equivalent to the LGS model (*n* = 0.5, *m* = 1, *E*<sub>0</sub> = 0.0 eV).<sup>26</sup> This type of fit *cannot* reproduce the data for reaction 8.

Assuming the neutral product of process 8 is H<sub>2</sub>CO, the threshold given in Table IV yields a Ni<sup>+</sup>-CH<sub>2</sub> bond energy of 3.31 ± 0.06 eV, in agreement with the result from reaction 2. Again, the error limits adequately include the possibility that the neutral products in reaction 8 are H<sub>2</sub> + CO. Note that the difference in bond energies, *D*<sup>0</sup>(CoCH<sub>2</sub><sup>+</sup>) - *D*<sup>0</sup>(NiCH<sub>2</sub><sup>+</sup>), determined in the ethylene oxide system, 0.10 eV, is identical with the difference determined in the cyclopropane system.

The final value for *D*<sup>0</sup>(NiCH<sub>2</sub><sup>+</sup>) is obtained from the average result of the c-C<sub>3</sub>H<sub>6</sub> and c-C<sub>2</sub>H<sub>4</sub>O systems, 3.26 ± 0.07 eV (75.2 ± 1.6 kcal/mol). Once again, this value is closer to the predicted value of ~72 kcal/mol<sup>2</sup> and well below the value obtained in previous ion beam studies, 3.75 ± 0.25 eV.<sup>4</sup> One major reason for the difference is because HAB assigned reaction 8 as exothermic. While this conclusion was reasonable given their data, the present results clearly show that this reaction is endothermic and thus that *D*<sup>0</sup>(Ni<sup>+</sup>-CH<sub>2</sub>) < 3.42 eV, outside the error limits of the HAB determination. Actually, HAB find a threshold for reaction 2 of 0.55 ± 0.3 eV. When corrected for the average electronic energy (0.05 eV for Ni<sup>+</sup>, Table I), the value of 0.6 ±

(23) We have previously measured such low thresholds in other systems, such as N<sup>+</sup> + H<sub>2</sub> (HD, D<sub>2</sub>), where the thermochemistry is reasonably well-known,<sup>7</sup> and Fe<sup>+</sup> + c-C<sub>2</sub>H<sub>2</sub>O system, a system similar to that treated here.<sup>18</sup>

(24) This value is based on a Maxwell-Boltzmann distribution of states given AB's cited filament temperature of 2500 K. While an explicit accounting of the various electronic states is desirable, this is not possible. The simple addition of the average electronic energy provides an approximate correction for the presence of excited state Co<sup>+</sup> ions in AB's beam.

(25) Forbes, R. A.; Lech, L. M.; Freiser, B. S. *Int. J. Mass Spectrom. Ion Processes* 1987, 77, 107-121.

(26) This model also includes a high-energy falloff beginning at 0.22 eV.<sup>13</sup>

TABLE V: Parameters Used in Eq 1 for Fitting Cu<sup>+</sup> Reaction Cross Sections

ionic product	<i>n</i>	<i>E</i> <sub>0</sub> , eV	<i>σ</i> <sub>0</sub>	<i>p</i>	<i>E</i> <sub>D</sub>
Cyclopropane					
CuCH <sub>2</sub> <sup>+</sup>	1.7 ± 0.1	1.84 ± 0.09	3.56 ± 0.48	1	4.0
CuC <sub>2</sub> H <sub>2</sub> <sup>+</sup>	2.2 ± 0.2	0.80 ± 0.10	0.04 ± 0.02		
CuC <sub>2</sub> H <sub>4</sub> <sup>+</sup>	1.8 ± 0.3	2.89 ± 0.11	0.76 ± 0.17	1	4.5
C <sub>3</sub> H <sub>3</sub> <sup>+</sup>	1.4 ± 0.1	2.31 ± 0.06	0.67 ± 0.07	1	3.8
C <sub>3</sub> H <sub>3</sub> <sup>+</sup>	1.6 ± 0.1	3.65 ± 0.14	0.80 ± 0.05	1	5.5
Ethylene Oxide					
CuCH <sub>2</sub> <sup>+</sup>	0.8 ± 0.1	0.65 ± 0.04	3.49 ± 0.51	1	4.0
<i>m/z</i> 91	1.2 ± 0.2	0.62 ± 0.06	0.26 ± 0.05		
CuCH <sub>2</sub> O <sup>+</sup>	1.9 ± 0.2	1.80 ± 0.10	0.20 ± 0.05	2	4.1

0.3 eV is in reasonable agreement with our determination of 0.78 ± 0.07 eV. HAB also determined *D*<sup>0</sup>(Ni<sup>+</sup>-CH<sub>2</sub>) = 4.1 ± 0.3 eV from analysis of the reaction of Ni<sup>+</sup> with ethene. They rejected this value, since the endothermicity of reaction 2 shows clearly that *D*<sup>0</sup>(NiCH<sub>2</sub><sup>+</sup>) < 3.99 eV, but this high value influenced them to choose a final bond energy of 3.75 eV, from an average of the 3.45 eV bond energy determined from reaction 2 and the upper limit of 3.99 eV. Work in our laboratories has shown that thermochemical analysis of metal ion reactions with ethene is difficult.<sup>9a</sup> Here, this is nicely demonstrated by the results of HAB who find that the ethene results suggest *D*<sup>0</sup>(Co<sup>+</sup>-CH<sub>2</sub>) is less than *D*<sup>0</sup>(Ni<sup>+</sup>-CH<sub>2</sub>) by 0.3 eV, in striking contrast to the results of the present study.

**Copper Methylidene Ion.** For reaction 2, the CuCH<sub>2</sub><sup>+</sup> cross section is similar in shape to that for NiCH<sub>2</sub><sup>+</sup>, Figure 3, and, therefore, is analyzed analogously. The model uses the parameters of Table V and reproduces the data very nicely, as shown in Figure 3. The threshold derived with this analysis results in *D*<sup>0</sup>(Cu<sup>+</sup>-CH<sub>2</sub>) = 2.15 ± 0.10 eV. In the ethylene oxide system, analysis of reaction 8 with M = Cu is achieved using the parameters given in Table V. This results in a Cu<sup>+</sup>-CH<sub>2</sub> bond energy of 2.77 ± 0.07 eV, much higher than the value from the c-C<sub>3</sub>H<sub>6</sub> system.

The obvious explanation for this discrepancy is that there is a barrier to the reaction in the cyclopropane system. It is also possible that the reaction 2 cross section rises slowly from the true thermodynamic threshold, although the apparent threshold of 1.4 eV is still 0.2 eV above the value suggested by *D*<sup>0</sup>(Cu<sup>+</sup>-CH<sub>2</sub>) = 2.77 eV. We reject the possibility that the threshold for reaction 8 be anomalously low since there are no excited states which could account for such an effect and the parameters used to analyze reaction 8 are such that the threshold is already at the highest plausible energy.<sup>27</sup> Confidence in the analysis of the cross section for reaction 8 is bolstered by noting that the parameters, Table V, are similar to those for CoCH<sub>2</sub><sup>+</sup> in the c-C<sub>3</sub>H<sub>6</sub> system, Table III, consistent with the similar shapes of the cross sections, Figures 1a and 2c. Indeed, the differences in these cross sections at low energies can be attributed to the various excited states and *J* levels populated for Co<sup>+</sup> vs the single electronic level populated for Cu<sup>+</sup>.

The final value for *D*<sup>0</sup>(CuCH<sub>2</sub><sup>+</sup>) is taken to be the value derived in the ethylene oxide system *D*<sup>0</sup>(CuCH<sub>2</sub><sup>+</sup>) = 2.77 ± 0.07 (63.9 ± 1.16 kcal/mol). No previous values exist for comparison although recent results from our laboratory speculated that *D*<sup>0</sup>-(Cu<sup>+</sup>-CHCH<sub>3</sub>) ≈ 36 kcal/mol.<sup>28</sup> While our present value seems high at first, it is in reasonable correspondence with the periodic trends correlation of ref 2.<sup>29</sup> Although this agreement suggests a covalent double bond, another possible structure for the CuCH<sub>2</sub><sup>+</sup> molecule is a dative interaction in which CH<sub>2</sub>(<sup>1</sup>A<sub>1</sub>) donates its lone pair of electrons into the empty 4s orbital of Cu<sup>+</sup>(<sup>1</sup>S, 3d<sup>10</sup>). This electronic structure would be nearly equivalent to a single M-C bond which have been found to have strengths of about 58

(27) The parameters used to analyze this reaction include a low value of *n* which means that the cross section rises very rapidly from the threshold. This leads to a threshold well above the apparent threshold.

(28) Georgiadis, R.; Fisher, E. R.; Armentrout, P. B. *J. Am. Chem. Soc.* **1989**, *111*, 4251-4262.

(29) This correlation suggests a Cu<sup>+</sup>-CH<sub>2</sub> bond strength of ~58 kcal/mol, since Cu<sup>+</sup> has a promotion energy of 3.03 eV.

TABLE VI: Summary of Bond Energies (eV) at 298 K<sup>a</sup>

<i>D</i> <sup>0</sup>	M = Co	M = Ni	M = Cu
M <sup>+</sup> -CH <sub>2</sub>	3.36 (0.07) 3.7 (0.3) <sup>b</sup> 3.65 (0.2) <sup>d</sup> 3.5 (0.3) <sup>e</sup>	3.26 (0.07) 3.75 (0.25) <sup>c</sup>	2.77 (0.07)
M <sup>+</sup> -C <sub>2</sub> H <sub>4</sub>	>1.73 (0.20) 2.0 (0.4) <sup>f</sup>	>1.51 (0.21) 2.1 (0.4) <sup>f</sup>	>1.13 (0.11) >1.2 (0.05) <sup>g</sup>
M <sup>+</sup> -C <sub>2</sub> H <sub>2</sub>	>1.47 (0.15)	>1.30 (0.09)	>1.32 (0.10) 1.13 (0.11)
M <sup>+</sup> -CH <sub>2</sub> O			
M <sup>+</sup> -O	3.30 (0.07) 3.36 (0.06) <sup>h</sup> 2.76 (0.10) <sup>i</sup>	2.86 (0.08) 2.79 (0.07) <sup>h</sup> 1.95 (0.10) <sup>i</sup>	1.67 (0.15) <sup>h</sup>
M-O	2.5 (0.1) 3.8 (0.2) <sup>j</sup>	2.6 (0.2) 3.6 (0.2) <sup>k</sup>	
M-H	2.02 (0.14) 1.95 <sup>l</sup>	2.58 (0.16) 2.69 <sup>l</sup>	2.67 (0.18) 2.64 <sup>l</sup>
	1.95 (0.13) <sup>m</sup>	2.56 (0.09) <sup>m</sup>	2.6 (0.04) <sup>m</sup> 2.7 (0.04) <sup>n</sup>

<sup>a</sup>Unless specified otherwise, the values are from this work. See text for discussion. Uncertainties are given in parentheses. <sup>b</sup>Reference 3. <sup>c</sup>Reference 4. <sup>d</sup>Reference 5. <sup>e</sup>Reference 25. <sup>f</sup>Reference 21. <sup>g</sup>Reference 31. <sup>h</sup>Reference 33. <sup>i</sup>Reference 34. <sup>j</sup>Reference 35. <sup>k</sup>Reference 36. <sup>l</sup>Bauschlicher, C. W.; Langhoff, S. R.; Partridge, H.; Barnes, L. A. *J. Chem. Phys.* **1989**, *91*, 2399-2411. <sup>m</sup>Kant, A.; Moon, K. A. *High Temp. Sci.* **1981**, *14*, 23; **1979**, *11*, 55. <sup>n</sup>Huber, K. P.; Herzberg, G. *Molecular Spectra and Molecular Structure IV. Constants of Diatomic Molecules*; Van Nostrand Reinhold: New York, 1979.

kcal/mol. Either electronic structure is roughly consistent with the bond energy determined here and it seems likely that a mixture of these configurations could be involved.

**Periodic Trends in *D*<sup>0</sup>(MCH<sub>2</sub><sup>+</sup>).** The M-CH<sub>2</sub><sup>+</sup> bond energies reported here resolve the discrepancy with the promotion energy correlation for M = Co and Ni. Although the values determined here are slightly higher than the predicted ~72 kcal/mol, they are in much better agreement with the periodic trends correlations than the previously reported 85 and 86 kcal/mol. The new value reported here for CuCH<sub>2</sub><sup>+</sup> is also in reasonable agreement with this correlation, as noted above. Given these new values of *D*<sup>0</sup>(MCH<sub>2</sub><sup>+</sup>) and others recently compiled for all of the first-row transition metals, we have reanalyzed the periodic trends in these bond energies. We find and report elsewhere that the promotion energy-bond strength correlation is indeed maintained with double bonds as well as single bonds of transition metals.<sup>30</sup>

**Metal Ethene and Metal Ethyne Ions.** Reaction 3, formation of MC<sub>2</sub>H<sub>4</sub><sup>+</sup> from c-C<sub>3</sub>H<sub>6</sub> is seen with all three metal ions. The thresholds for MC<sub>2</sub>H<sub>4</sub><sup>+</sup> listed in Tables III-V lead to the bond energies of Table VI. For Co<sup>+</sup> and Ni<sup>+</sup>, these values are somewhat lower than previously reported values, *D*<sup>0</sup>(Co<sup>+</sup>-C<sub>2</sub>H<sub>4</sub>) = 2.0 ± 0.4 eV and *D*<sup>0</sup>(Ni<sup>+</sup>-C<sub>2</sub>H<sub>4</sub>) = 2.1 ± 0.4 eV,<sup>21</sup> but are within the combined error limits of these values. This suggests that the best values for *D*<sup>0</sup>(Co<sup>+</sup>-C<sub>2</sub>H<sub>4</sub>) and *D*<sup>0</sup>(Ni<sup>+</sup>-C<sub>2</sub>H<sub>4</sub>) may be ~1.9 and ~1.7 eV, respectively. For M = Cu, the value derived here is also in reasonable agreement with a previous limit of *D*<sup>0</sup>(Cu<sup>+</sup>-CH<sub>2</sub>) > 1.2 ± 0.05 eV.<sup>31</sup> The values derived here should be viewed with some caution, however, since formation of MC<sub>2</sub>H<sub>4</sub><sup>+</sup>, reaction 3, competes strongly with the energetically more favorable formation of MCH<sub>2</sub><sup>+</sup> and MC<sub>2</sub>H<sub>2</sub><sup>+</sup>. This strong competition could cause a delayed onset for the MC<sub>2</sub>H<sub>4</sub><sup>+</sup> product, leading to bond energies which are lower limits.

MC<sub>2</sub>H<sub>2</sub><sup>+</sup> is formed in the cyclopropane system, reaction 4, for all three metal ions and in the ethylene oxide system, reaction 12, for M = Co and Ni. In the ethylene oxide systems, reaction 12 is exothermic for both Co<sup>+</sup> and Ni<sup>+</sup>, which provides a lower limit of 0.39 ± 0.01 eV for *D*<sup>0</sup>(M<sup>+</sup>-C<sub>2</sub>H<sub>2</sub>) assuming that the neutral product is H<sub>2</sub>O. Analyses of reaction 4, Tables III-V, yield thresholds which correspond to the bond energies given in Table

(30) Armentrout, P. B.; Sunderlin, L. S.; Fisher, E. R. *Inorg. Chem.*, in press.

(31) Burnier, R. C.; Byrd, G. D.; Freiser, B. S. *Anal. Chem.* **1980**, *52*, 1641-1650.

VI, if the neutral product is  $\text{CH}_4$ . This is a reasonable assumption since the  $\text{MC}_2\text{H}_2^+$  product has a lower threshold than  $\text{MC}_2\text{H}_4^+$ , indicating that it is not the decomposition product of  $\text{MC}_2\text{H}_4^+$ , i.e.,  $\text{MC}_2\text{H}_2^+ + \text{H}_2$ . In all three systems, if the neutral products are assumed to be  $(\text{O} + \text{H}_2)$  or  $(\text{CH}_2 + \text{H}_2)$ , the resulting bond energies are  $\geq 5$  eV, values which are excessively large. As in the case of  $\text{M}^+-\text{C}_2\text{H}_4$ , these reactions are in competition with  $\text{MCH}_2^+$  formation which means that the bond energies derived here could be simply lower limits. Other  $\text{M}^+-\text{C}_2\text{H}_2$  bond energies available for comparison are  $D^\circ(\text{Cr}^+-\text{C}_2\text{H}_2) = 2.1 \pm 0.2$  eV<sup>16</sup> and  $D^\circ(\text{V}^+-\text{C}_2\text{H}_2) = 2.2 \pm 0.2$  eV.<sup>32</sup>

Process 16, formation of  $\text{MCH}_2\text{O}^+$ , is only seen with  $\text{M} = \text{Cu}$ . Analysis of the reaction cross section for this reaction, Table V, leads to  $D^\circ(\text{Cu}^+-\text{CH}_2\text{O}) = 2.19 \pm 0.11$  eV. This value is higher than the value derived above for  $D^\circ(\text{Cu}^+-\text{C}_2\text{H}_4) = 1.13 \pm 0.11$  eV, which could be due to interaction with the oxygen lone pair electrons.

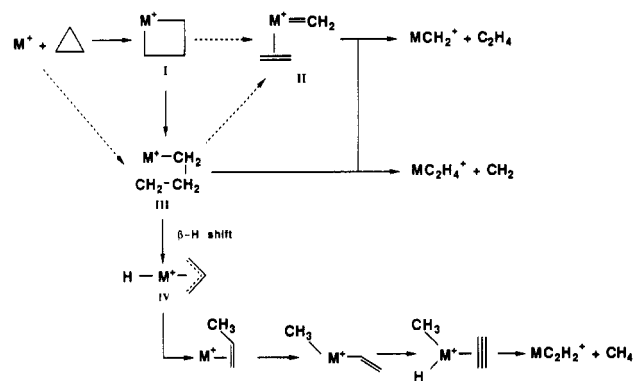
**Metal Oxide Ion and Neutral.** In the reaction with ethylene oxide, formation of  $\text{MO}^+$  is endothermic for both  $\text{Co}^+$  and  $\text{Ni}^+$  but is not observed at any energies for  $\text{Cu}^+$ . Analysis of reaction 13 for  $\text{M} = \text{Co}$  yields a threshold of  $0.37 \pm 0.04$  eV (Table III). This confirms that reaction of  $\text{Co}^+(\text{a}^5\text{F})$  to form  $\text{CoO}^+$  should be exothermic, which explains why the cross section is nonzero at the lowest kinetic energies, Figure 2a. This threshold leads to a  $\text{Co}^+-\text{O}$  bond energy of  $3.30 \pm 0.07$  eV, in good agreement with that obtained from the reaction of  $\text{Co}^+$  with  $\text{O}_2$ ,  $3.36 \pm 0.06$  eV.<sup>33</sup> Analysis of reaction 13 with  $\text{M} = \text{Ni}$  yields a threshold, Table IV, which leads to a  $\text{Ni}^+-\text{O}$  bond energy of  $2.86 \pm 0.08$  eV. This value is in excellent agreement with the bond energy obtained from the reaction of  $\text{Ni}^+ + \text{O}_2$ ,  $2.79 \pm 0.07$  eV.<sup>33</sup> These bond energies are higher than those derived from a similar study.<sup>34</sup> A comparison of these results will be discussed in detail in a forthcoming paper.<sup>33</sup>

In the reaction of  $\text{M}^+$  ( $\text{M} = \text{Co}, \text{Ni}$ ) with ethylene oxide,  $\text{C}_2\text{H}_4\text{O}^+$  is observed as a minor endothermic product at higher energies. (While it is possible that ions at this mass are actually  $\text{CO}^+$ , this implies the concomitant formation of  $\text{MCH}_4$  which seems unlikely.) Analysis of the cross section for  $\text{M} = \text{Co}$  yields a threshold of  $3.78 \pm 0.08$  eV, Table III, which leads to  $D^\circ(\text{CoO}) = 2.5 \pm 0.1$  eV. For  $\text{M} = \text{Ni}$ , the  $\text{C}_2\text{H}_4\text{O}^+$  product has a threshold, Table IV, which yields  $D^\circ(\text{NiO}) = 2.6 \pm 0.2$  eV. These neutral metal oxide bond values should be considered as lower limits since the thresholds may be too high due to competition with process 13 and other reactions. This possibility seems confirmed by the observation that the values derived here are considerably lower than literature values of  $D^\circ(\text{Co}-\text{O}) = 3.8 \pm 0.2$  eV<sup>35</sup> and  $D^\circ(\text{Ni}-\text{O}) = 3.6 \pm 0.2$  eV.<sup>36</sup>

**Metal Hydride Ion and Neutral.** Formation of  $\text{MH}^+$  is only seen in the  $\text{Co}^+$  + cyclopropane system, reaction 5. Analysis of this process, Table III, leads to a  $\text{Co}^+-\text{H}$  bond energy of  $1.83 \pm 0.15$  eV ( $42 \pm 4$  kcal/mol), if we assume the neutral  $\text{C}_3\text{H}_5$  fragment retains its cyclic structure. This value is in fairly good agreement with that found in the reaction of  $\text{Co}^+ + \text{H}_2$ ,  $D^\circ(\text{CoH}^+) = 2.02 \pm 0.06$  eV ( $46.6 \pm 1.4$  kcal/mol).<sup>37</sup> This confirms the identity of the neutral radical since production of an allyl radical would lead to a threshold 1.2 eV lower (Table II).

The alkyl ions formed in the reactions of  $\text{M}^+$  ( $\text{M} = \text{Co}, \text{Ni}$ , and  $\text{Cu}$ ) with cyclopropane are  $\text{C}_3\text{H}_5^+$  and  $\text{C}_3\text{H}_3^+$ . As stated previously, formation of  $\text{C}_3\text{H}_3^+$  is most likely due to subsequent loss of  $\text{H}_2$  from  $\text{C}_3\text{H}_5^+$ . This is confirmed by the observation that, with  $\text{M} = \text{Co}$ , the sum of the  $\text{C}_3\text{H}_5^+$  cross sections is exactly the same shape as the slightly larger  $\text{CoH}^+$  cross section. Threshold analyses of both alkyl products with the three metal ions are listed

## SCHEME I



in Tables III-V. From these, we derive neutral MH bond energies of  $D^\circ(\text{Co}-\text{H}) = 2.02 \pm 0.14$  eV ( $47 \pm 3$  kcal/mol),  $D^\circ(\text{Ni}-\text{H}) = 2.73 \pm 0.22$  eV ( $63 \pm 5$  kcal/mol), and  $D^\circ(\text{Cu}-\text{H}) = 2.75 \pm 0.14$  eV ( $63 \pm 3$  kcal/mol), again assuming that the  $\text{C}_3\text{H}_5^+$  fragment has retained its cyclic structure. This assumption is apparently justified since these MH bond energies are all in good agreement with a recent study where these bond energies were determined from reactions of the metal ions with alkanes,<sup>28</sup>  $D^\circ(\text{CoH}) = 46 \pm 3$  kcal/mol,  $D^\circ(\text{NiH}) = 58 \pm 3$  kcal/mol, and  $D^\circ(\text{CuH}) = 61 \pm 4$  kcal/mol. If the  $\text{C}_3\text{H}_5^+$  ion were actually the allyl ion, this would lead to MH bond energies which are lower by 29 kcal/mol.<sup>38</sup> Because of this good agreement, we average the present results for  $D^\circ(\text{MH})$  with those from the earlier study (which came from results of reactions with ethane, propane, and isobutane). This leads to the slightly revised values given in Table VI.

In the ethylene oxide systems, production of  $\text{MH} + \text{C}_2\text{H}_3\text{O}^+$  is observed to be exothermic for all three metals. This is consistent with the MH bond energies from ref 28 since these values imply that this reaction is exothermic by about 0.3, 0.6, and 0.8 eV for Co, Ni, and Cu, respectively. This assumes that the ionic product is the acetyl ion, rather than cyclic  $\text{C}_2\text{H}_3\text{O}^+$ . The latter product leads to endothermic production of MH with calculated thresholds of 1.7, 1.4, and 1.2 eV, respectively. This process may explain the features in the  $\text{C}_2\text{H}_3\text{O}^+$  cross sections observed at high energies in the  $\text{Co}^+$  and  $\text{Ni}^+$  systems (Figure 2, a and b). Thus, in contrast to the cyclopropane system where the cyclic structure is retained when  $\text{H}^+$  is removed by the metal ion, this process leads to extensive rearrangement in the ethylene oxide system.

## Discussion

**Reaction Mechanism: Cyclopropane.** The generally accepted mechanism for reaction of metal ions with cyclopropane entails C-C bond activation to form the metallacyclobutane ion I, Scheme I.<sup>3,16</sup> Cleavage across the metallacycle yields intermediate II, which can lose ethene, reaction 2, or  $\text{CH}_2$ , reaction 3.

While this scheme is attractive in its simplicity, conversion of I to II is a (2 + 2) reaction, ordinarily forbidden by Woodward-Hoffman orbital symmetry rules. Other similar (2 + 2) reactions such as four-center dehydrogenation of methane and  $\beta$ -hydrogen migration have also been seen for transition-metal ions. Such reactions occur readily for early transition-metal ions,  $\text{Sc}^+-\text{Cr}^+$ ; but for late transition-metal ions,  $\text{Mn}^+-\text{Cu}^+$ , dehydrogenation of methane is not seen, and for some of the late transition-metal ions, there is a barrier to dehydrogenation of ethane, potentially indicating a barrier to  $\beta$ -hydrogen migration. Theoretical considerations maintain that these concerted reactions become orbitally allowed when the bonding involves metal orbitals having primarily d character.<sup>39</sup> The differences in reactivity between early and late transition-metal ions can be explained by noting that the late metal ions have substantially more s character

(32) Aristov, N.; Armentrout, P. B. *J. Am. Chem. Soc.* **1986**, *108*, 1806-1819.

(33) Fisher, E. R.; Elkind, J. L.; Armentrout, P. B., work in progress.

(34) Armentrout, P. B.; Halle, L. F.; Beauchamp, J. L. *J. Chem. Phys.* **1982**, *76*, 2449-2457.

(35) Smoes, S.; Mandy, F.; Auwera-Mahieu, A.; Drowart, J. *Bull. Soc. Chim. Belg.* **1972**, *81*, 45.

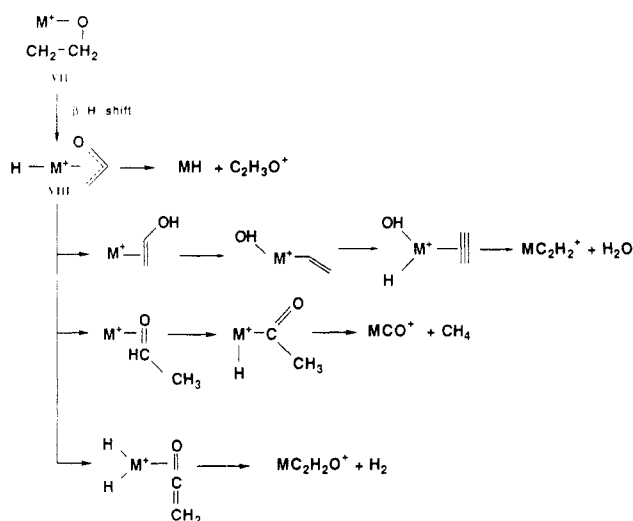
(36) Farber, M.; Srivastava, R. D. *Anal. Calorimetry* **1974**, *3*, 731-741.

(37) Elkind, J. L.; Armentrout, P. B. *J. Phys. Chem.* **1986**, *90*, 6576-6586.

(38) Lias, S. G.; Bartmess, J. E.; Liebman, J. F.; Holmes, J. L.; Levin, R. D.; Mallard, W. G. *J. Phys. Chem. Ref. Data* **1988**, *17*, Suppl. No. 1.

(39) Steigerwald, M. L.; Goddard, W. A. *J. Am. Chem. Soc.* **1984**, *106*, 308-311.

## SCHEME II



to their bonding than the early metal ions. This argument has been detailed for reactions of  $\text{Mn}^+$  with cyclopropane and ethylene oxide.<sup>17</sup>

An alternative mechanism which we have suggested<sup>17</sup> for the late transition metals is also shown in Scheme I. This mechanism involves formation of radical III,  $\text{M}^+ - \text{CH}_2\text{CH}_2\text{CH}_2^*$ , either directly from reactants or from I followed by cleavage of one of the M-C bonds. Cleavage of the  $\alpha$ -C-C bond in III leads to  $\text{MCH}_2^+$  formation (possibly through II), while cleavage of the  $\beta$ -C-C bond yields  $\text{MC}_2\text{H}_4^+$ . If the M-C bond in III has a bond strength equivalent to  $D^\circ(\text{M}^+ - \text{CH}_3)$ , then this intermediate lies 0.48, 0.65, and 1.3 eV above the reactants for  $\text{M} = \text{Co}, \text{Ni},$  and  $\text{Cu}$ , respectively. While these energies lie below the threshold for reaction 2 in the Co and Ni systems, the thermodynamic threshold in the Cu system is 1.2 eV. Thus, this mechanism could explain the barrier in excess of the endothermicity observed for reaction 2 with  $\text{M} = \text{Cu}$ .

A natural mechanism for formation of  $\text{MC}_2\text{H}_2^+$ , reaction 4, is subsequent dehydrogenation of  $\text{MC}_2\text{H}_4^+$ ; however, thermochemical arguments indicate that  $\text{CH}_4$  must be the neutral product for this process. This clearly involves extensive rearrangement, indicating a high level of hydrogen mobility. A possible mechanism for this process is included in Scheme I.<sup>40</sup> This type of mechanism is consistent with elevated thresholds for reaction 12 since elimination of  $\text{CH}_4$  must compete with propene loss from intermediate IV, a much more favorable process thermodynamically.

Reactions 5-7 involve the activation of a C-H bond of  $c\text{-C}_3\text{H}_6$ . Comparison of cross-section magnitudes, Figure 1, shows that this is clearly a less favorable step than C-C activation. The thermochemistry of these processes indicate that the cyclic structure of  $\text{C}_3\text{H}_5$  and  $\text{C}_3\text{H}_5^+$  is retained in these reactions. Competition between reactions 5 and 6 is driven by the relative ionization potentials of MH and  $c\text{-C}_3\text{H}_5$ , such that the  $\text{MH}^+$  product is observed only in the case of Co. This is verified by noting that  $\text{IP}(\text{Co}-\text{H}) < \text{IP}(c\text{-C}_3\text{H}_5)$ , whereas the IPs of NiH and CuH exceed that of  $c\text{-C}_3\text{H}_5$  by at least 0.3 eV.<sup>41</sup> Similar results were observed for reaction of  $\text{Co}^+, \text{Ni}^+,$  and  $\text{Cu}^+$  with alkanes.<sup>28</sup>

**Reaction Mechanism: Ethylene Oxide.** In analogy with the  $c\text{-C}_3\text{H}_6$  system, reaction of metal ions with  $c\text{-C}_2\text{H}_4\text{O}$  is generally believed to proceed via the metallacycle intermediates V and VI.<sup>4,16,42</sup> Intermediate V can account for reactions 8, 10, 13, 14,



and 16, while VI could also contribute to reactions 8 and 16. Again, however, these reactions are usually envisioned as (2 + 2) cleavages across the metallacycle. Alternatively, a radical intermediate analogous to III may be formed,  $\text{M}^+ - \text{OCH}_2\text{CH}_2^*$ , VII, Scheme II, but now the M-O bond can be much stronger than the M-C bond due to favorable interactions of the oxygen lone pairs. For example,  $D^\circ(\text{Co}^+ - \text{OH})^{43}$  exceeds  $D^\circ(\text{Co}^+ - \text{CH}_3)^{28}$  by  $0.95 \pm 0.20$  eV. This presumably lowers the energy of the radical intermediate enough that no barriers are observed for the reactions of  $\text{M}^+$  with  $c\text{-C}_2\text{H}_4\text{O}$  with any metal.

The proposed radical intermediate VII also offers a viable mechanism for reactions 9, 11, 12, and 15 (Scheme II). These processes involve extensive rearrangement, suggesting that the H atoms are quite mobile and are much like the analogous reaction 4 in the cyclopropane system. Previously, the mechanism for these reactions has been suggested to be metal-induced rearrangement of  $c\text{-C}_2\text{H}_4\text{O}$  to acetaldehyde, but the mechanism of this rearrangement was not specified.<sup>4</sup> Scheme II suggests that this transformation occurs via a  $\beta$ -H transfer from VII to form VIII. This intermediate is equivalent to that formed by insertion of  $\text{M}^+$  into one of the terminal C-H bonds of acetaldehyde and to a hydrido-enol metal ion. Finally, we note that observation of the long-lived adduct species in the  $\text{Co}^+$  and  $\text{Ni}^+$  systems is consistent with the formation of intermediates which require extensive rearrangement to reform reactants. Indeed, in order to be observed, these intermediates must have a lifetime which exceeds the flight time to the detector,  $\sim 300 \mu\text{s}$  at a kinetic energy of 0.1 eV. Such long-lived species are unusual but not unprecedented. For instance, Tolbert and Beauchamp have characterized long-lived intermediates in the reactions of  $\text{Ti}^+$  and  $\text{V}^+$  with  $n$ -butanes,<sup>44</sup> and we have recently observed a five-atom intermediate which lives in excess of  $\sim 60 \mu\text{s}$ .<sup>45</sup>

**Reactivity of  $\text{Cu}^+$ .** The reactions of  $\text{Cu}^+$  (a closed-shell  $3d^{10}$  ion) with cyclopropane are very similar to those of  $\text{Co}^+$  and  $\text{Ni}^+$ . This surprising result agrees with the finding of Elkind and Armentrout<sup>37</sup> that  $\text{Co}^+, \text{Ni}^+,$  and  $\text{Cu}^+$  have very similar reactivity with  $\text{H}_2$ . In a study of the reactivity of these three metal ions with noncyclic alkanes,<sup>28</sup>  $\text{Cu}^+$  exhibited none of the exothermic behavior observed for  $\text{Co}^+$  and  $\text{Ni}^+$ , but the endothermic reactions of all three ions were very similar. Presumably, the interactions of  $\text{Cu}^+$  with C-H and C-C bonds is accompanied by significant activation barriers which prevent the exothermic reactions but still allow the endothermic ones. In the present study, this is evident in the cyclopropane system, where we observe a barrier in excess of the endothermicity of reaction 2.

In the ethylene oxide system, the reactivity of  $\text{Cu}^+$  differs greatly from that of  $\text{Co}^+$  and  $\text{Ni}^+$ . At low energies, the latter two metal ions react to form a multitude of products, while  $\text{Cu}^+$  forms only the acetyl ion,  $\text{CH}_3\text{CO}^+$ . Unlike reaction 11, reactions 9, 12, and 15 (the other processes observed to be exothermic for  $\text{Co}^+$  and  $\text{Ni}^+$ ) involve intermediates containing two covalent bonds to the metal ion (Scheme II). As with the alkanes, such intermediates should lead to significant activation barriers with  $\text{Cu}^+$  such that these three exothermic reactions are not observed. Indeed, reaction 9, formation of  $\text{CuCO}^+$  (product  $m/z$  91), is observed to have a barrier of 0.6 eV. [As noted above, this product could also be  $\text{CuC}_2\text{H}_4^+$ , but this threshold would lead to a bond energy for  $\text{Cu}^+ - \text{C}_2\text{H}_4$  of 3.0 eV, a value well above those measured for other metals.] In contrast, no such constraint is encountered for reaction 11 and since there are no competing exothermic channels, the cross section for the exothermic formation of the acetyl ion is greatest with  $\text{M} = \text{Cu}$ . This process is particularly favorable because it

(40) This mechanism also suggests that methane elimination should be observed as a high-energy process in the reaction of  $\text{M}^+$  with propene. Such reactions have not been studied as of yet, although the analogous process has been seen at high energies in the reaction of  $\text{Co}^+$  with isobutene. Armentrout, P. B.; Halle, L. F.; Beauchamp, J. L. *J. Am. Chem. Soc.* **1981**, *103*, 6624-6628.

(41) Based on thermochemistry given in Table II and ref 28.

(42) Kang, H.; Beauchamp, J. L. *J. Am. Chem. Soc.* **1986**, *108*, 5663-5668.

(43) Cassidy, C. J.; Freiser, B. S. *J. Am. Chem. Soc.* **1984**, *106*, 6176-6179.

(44) Tolbert, M. A.; Beauchamp, J. L. *J. Am. Chem. Soc.* **1986**, *108*, 7509-7517.

(45) Clemmer, D. E.; Armentrout, P. B. *J. Am. Chem. Soc.* **1989**, *111*, 8280-8281.

is accompanied by formation of the stable neutral species  $\text{CuH}^+$  ( $^1\Sigma^+$ ). Close examination of the cross section for this process shows that it has a second feature which begins at  $\sim 0.3$  eV (Figure 2c). This feature could be the result of formation of a different structure for the  $\text{C}_2\text{H}_3\text{O}^+$  ion, either  $\text{CH}_2=\text{COH}^+$  or the cyclic species, both of which should be formed in endothermic reactions.

Of the three metal ions studied here,  $\text{Cu}^+$  is the only one which reacts with ethylene oxide to form  $\text{MCH}_2\text{O}^+$  (reaction 16). The cross section for this product, however, is very small since it competes directly with formation of the thermodynamically favored  $\text{CuCH}_2^+$ . In the Co and Ni systems, this product may not be observed simply because there are many more competing channels.

### Summary

The reactions of  $\text{Co}^+$ ,  $\text{Ni}^+$ , and  $\text{Cu}^+$  with *c*- $\text{C}_3\text{H}_6$  and *c*- $\text{C}_2\text{H}_4\text{O}$  are studied by using guided ion beam mass spectrometry. Revised bond energies are found for  $D^\circ(\text{Co}^+-\text{CH}_2)$  and  $D^\circ(\text{Ni}^+-\text{CH}_2)$  and a new value for  $D^\circ(\text{Cu}^+-\text{CH}_2)$  is reported. These are listed in Table VI. It is shown that these values are more reliable than those determined previously and that they are in better agreement with the periodic trends correlation of ref 2. Further, these values lead to a more comprehensive periodic trends analysis detailed elsewhere.<sup>30</sup>

In addition to the bond energies for  $\text{MCH}_2^+$ , we also evaluate values for  $D^\circ(\text{M}-\text{H})$ , where  $\text{M} = \text{Co}, \text{Ni}, \text{and Cu}$ ;  $D^\circ(\text{M}^+-\text{O})$  and  $D^\circ(\text{M}-\text{O})$  where  $\text{M} = \text{Co}$  and  $\text{Ni}$ ; as well as lower limits to both  $D^\circ(\text{M}^+-\text{C}_2\text{H}_4)$  and  $D^\circ(\text{M}^+-\text{C}_2\text{H}_2)$  for all three metal ions. These are included in Table VI. The bond energies derived here for the MH species agree well with the results of another recent study<sup>28</sup> and are used to revise our suggested values for  $D^\circ(\text{M}-\text{H})$ . Likewise, the  $\text{MO}^+$  bond energies for  $\text{M} = \text{Co}$  and  $\text{Ni}$  are in good agreement with values derived from the reaction of  $\text{M}^+$  with  $\text{O}_2$ .<sup>33</sup>

The reaction mechanism for the interaction of metal ions with these cyclic compounds is discussed in some detail. An alternative to the commonly assumed mechanism is suggested which can also explain several minor reactions observed in these studies. This mechanism also provides an explanation for the observation of an activation barrier in excess of the reaction endothermicity for formation of  $\text{CuCH}_2^+$  from cyclopropane.

**Acknowledgment.** This work was funded by the National Science Foundation, Grant No. CHE-8796289.

**Registry No.**  $\text{Co}^+$ , 16610-75-6;  $\text{Ni}^+$ , 14903-34-5;  $\text{Cu}^+$ , 17493-86-6;  $\text{CoCH}_2^+$ , 76792-07-9;  $\text{CoC}_2\text{H}_3^+$ , 124687-61-2;  $\text{CoC}_2\text{H}_4^+$ , 124687-59-8;  $\text{CoH}^+$ , 12378-09-5;  $\text{CoO}^+$ , 60131-09-1;  $\text{NiCH}_2^+$ , 87453-14-3;  $\text{NiC}_2\text{H}_2^+$ , 124687-62-3;  $\text{NiC}_2\text{H}_4^+$ , 124687-60-1;  $\text{NiO}^+$ , 60131-11-5;  $\text{CuCH}_2^+$ , 117130-08-2;  $\text{CuC}_2\text{H}_2^+$ , 45326-64-5;  $\text{CuC}_2\text{H}_4^+$ , 67729-41-3;  $\text{CuCH}_2\text{O}^+$ , 124687-63-4; cyclopropane, 75-19-4; ethylene oxide, 75-21-8.

## Relative Partition Coefficients for Organic Solutes from Fluid Simulations

William L. Jorgensen,\* James M. Briggs, and M. Leonor Contreras†

Department of Chemistry, Purdue University, West Lafayette, Indiana 47907 (Received: June 16, 1989)

A procedure is noted for obtaining the difference in partition coefficients ( $\log P$ ) for two solutes between two solvents. Fluid simulations are required in which one solute is mutated to the other in both solvents, and the changes in free energies of solvation are computed. The method is illustrated for eight pairs of organic solutes partitioning between water and chloroform. Monte Carlo statistical mechanics simulations are used with statistical perturbation theory to calculate the requisite free energy changes. The results are compared with experimental  $\log P$  data and relative free energies of hydration. For the present solute pairs, the differences in partition coefficients are dominated by the differences in hydration. Such computations are useful for providing estimates of the effects of substituent changes on partitioning behavior and for further testing of intermolecular potential functions. The paper also contains previously unreported potential function parameters for acetic acid, methyl acetate, acetone, and pyrimidine and a summary of thermodynamics results for the corresponding pure liquids.

The distribution of an organic solute between water and non-polar media is an important parameter for structure-activity analyses in pharmacological research.<sup>1-3</sup> Many procedures have now been devised to estimate the logarithm of the partition coefficient ( $\log P$ ) for a solute between water and several solvents, especially 1-octanol.<sup>1-5</sup> These methods mostly feature additive schemes with atom and group increments or correlations involving solvent-accessible surface areas. The associated parameters have been selected to give the best fit to experimental  $\log P$  data. In the present paper, a more fundamental, theoretical approach to computing differences in partition coefficients is explored based on fluid simultaneous at the atomic level.

If one considers the thermodynamic cycle below for two solutes,



$$\Delta G_1(\text{A}) = -2.3RT \log P_A \quad (1)$$

$$\Delta G_1(\text{B}) = -2.3RT \log P_B \quad (2)$$

A and B, in two solvents,  $\log P$  for the solutes is defined in eq

1 and 2 in terms of the free energies of transfer. From the cycle, eq 3 is obtained which yields eq 4. The last expression associates

$$\Delta G_1(\text{B}) - \Delta G_1(\text{A}) = \Delta G_2(\text{AB}) - \Delta G_1(\text{AB}) \quad (3)$$

$$\Delta \log P = \log P_B - \log P_A = (\Delta G_1(\text{AB}) - \Delta G_2(\text{AB}))/2.3RT \quad (4)$$

the difference in  $\log P$ 's with the difference in free energies for mutating A to B in the two solvents. If contributions from internal degrees of freedom are ignored,  $\Delta G_1$  and  $\Delta G_2$  are just the difference in free energies of solvation for A and B. For example, if solvent 1 is water and solvent 2 is a nonpolar solvent, a positive  $\Delta \log P$  implies that the change from A to B results in greater affinity for the nonpolar solvent. This comes about by the change in solvation free energies for A going to B being less favorable in water than in the nonpolar solvent ( $\Delta G_1 > \Delta G_2$ ).

Fortunately for the present purposes,  $\Delta G_1$  and  $\Delta G_2$  are available from Monte Carlo or molecular dynamics simulations in which

(1) Leo, A.; Hansch, C.; Elkins, D. *Chem. Rev.* **1971**, *71*, 525.

(2) Hansch, C.; Leo, A. *Substituent Constants for Correlation Analysis in Chemistry and Biology*; Wiley: New York, 1979.

(3) *Partition Coefficient; Determination and Estimation*; Dunn, W. J., III, Block J. S., Pearlman, R. S., Eds.; Pergamon: New York, 1986.

(4) Dunn, W. J., III; Koehler, M. G.; Grigoras, S. *J. Med. Chem.* **1987**, *30*, 1121.

(5) Klopman, G.; Nambodiri, K.; Schochet, M. *J. Comput. Chem.* **1985**, *6*, 28.

\* Permanent address: Chemistry Department, University of Santiago de Chile, Santiago-2, Chile.